VOLUME 81 PAPER No. 776

PROCEEDINGS

AMERICAN SOCIETY OF CIVIL ENGINEERS

AUGUST, 1955

AMERICAN SOCIETY OF CIVIL ENGINEERS FOUNDED 1852

DISCUSSION OF PROCEEDINGS PAPERS

387, 528, 604, 607, 674

ENGINEERING MECHANICS DIVISION

Headquarters of the Society
33 W. 39th St.
New York 18, N. Y.

PRICE $0.50 PER COPY

Current discussion of papers sponsored by the Engineering Mechanics Division is presented as follows:

This paper was published at 1745 S. State Street, Ann Arbor, Mich., by the American Society of Civil Engineers. Editorial and General Offices are at 33 West Thirty-ninth Street, New York 18, N.Y.

Discussion of
"AN EXPERIMENTAL STUDY OF BUBBLES MOVING IN LIQUIDS"

by W. L. Haberman and R. K. Morton
(Proc. Paper 387)

W. L. HABERMAN[1] and R. K. MORTON.[2]—The discussion by Messrs. Roberson, Baker, and Ruff[3] has dealt with the upward and downstream motion of bubbles in horizontal pipes. The velocities of these bubbles are affected not only by the turbulence in the stream, but also by the velocity distribution in the pipe and by the proximity of the pipe walls. In addition, acceleration of the bubble in the downstream and upward direction takes place subsequent to release of the bubble. The velocities U and V of the equation[4] given by the discussers are, therefore, average velocities. Since effects as described above are included in the experimentally determined rise velocities in pipes, scatter in the results are to be expected. For the same reason, these velocities should not be compared quantitatively with those obtained for bubbles rising freely in a large quiet medium.

The discussers have commented on the absence of scatter in Figure 2. It had been observed during the experiments at the Taylor Model Basin that the velocities of large bubbles surrounded by smaller satellite bubbles differed somewhat from corresponding ones free of satellites. Hence, only the results for bubbles which were essentially free of satellites were included in the plot.

1. Physicist, David Taylor Model Basin, U. S. Dept. of the Navy, Washington, D. C.
2. Mathematician, David Taylor Model Basin, U. S. Dept. of the Navy, Washington, D. C.
3. Proc. Sep. 606
4. This equation for the travel (L) of the bubble should read $L = \frac{DV}{U}$.

Discussion of
"ANALOG COMPUTERS APPLIED TO ELASTIC-PLASTIC SYSTEMS"

by Leo Schenker and Gunther Martin
(Proc. Paper 528)

J. ARCHER,[1] J.M. ASCE, and A. LANGE.[2]—It is indeed a pleasure to see in this paper a further application of the analog computer to complicated non-linear problems. The analog computer has apparently unlimited fields of usefulness, one of which Mr. Schenker and Mr. Martin have clearly delineated here.

The Civil Engineering Department of Massachusetts Institute of Technology is engaged in the study of elastic-plastic problems like the one discussed in this paper. The following circuit has been devised to simulate the elastic-plastic phenomenon on a high-speed electronic computer, such as the General Purpose Simulator[3] at the Instrumentation Laboratory.

It should be noted that this circuit functions properly for both positive and negative values of x. Also, because this circuit is intended for use with high-speed computers it does not use relays as circuit elements. Elimination of the relays permits a more accurate representation of the elastic-plastic phenomenon, since the finite delays involved in the opening and closing of the relays are eliminated.

This circuit makes use of three standard analog computer devices—summing and inverting amplifiers, coefficient pots, and hysteresis units.

The algebraic expression describing the non-linear operation is quite cumbersome in this case; consequently, the operation of the circuit is analyzed here by considering wave forms at various points in the circuit. Figure 1 shows the circuit used. Figure 2 illustrated the waveforms which appear in various parts of this circuit, as designated by the lower case letters "a," "b," etc. In the case shown $k_1 = k_2 = k$. In all these diagrams x and R(x) are shown plotted against time t. Figure 3 shows R(x) plotted against x, with the Figures 1, 2, 3 etc. corresponding to $t = t_1$, $t = t_2$ etc.

The adjustment of the hysteresis unit determines the hysteresis dead-zone in terms of the percentage of the full-scale signal. Physically, this dead-zone is analogous to the elastic-limit deflection, or elastic-limit resistance, and the full scale signal is analogous to the maximum expected value of deflection, in accordance with the usual analog computer scaling techniques.

The relative values of k_1 and k_2 determine the character of the elastic-plastic resistance function. For example, when $k_1 = k_2$, the R(x) function is the same as that used by Mr. Schenker and Mr. Martin. The two cases for $k_1 > k_2$ and $k_1 < k_2$ are shown in Figure 4, labeled "a" and "b" respectively. Physically, these two cases represent a resistance which is at first elastic, then elastic and plastic, with a "slope" (elastic coefficient) of $(k_1 - k_2)$.

Theoretically, there is no limit to how complex the simulation may be. For example, there may be n hysteresis units in parallel, each with its own coefficient k_i and its own elastic limit x_{L_i}.

Another physically important factor is that of asymmetry. Either k or x_L may be different for $x > o$ or $x < o$. The simulation of this case is shown in Figure 5, using simple germanium diodes in shunt arrangement for rectifying.

1. Civ. Eng. Dept., Massachusetts Inst. of Technology, Cambridge, Mass.
2. Instrumentation Lab., Massachusetts Inst. of Technology, Cambridge, Mass.
3. Commercially available.

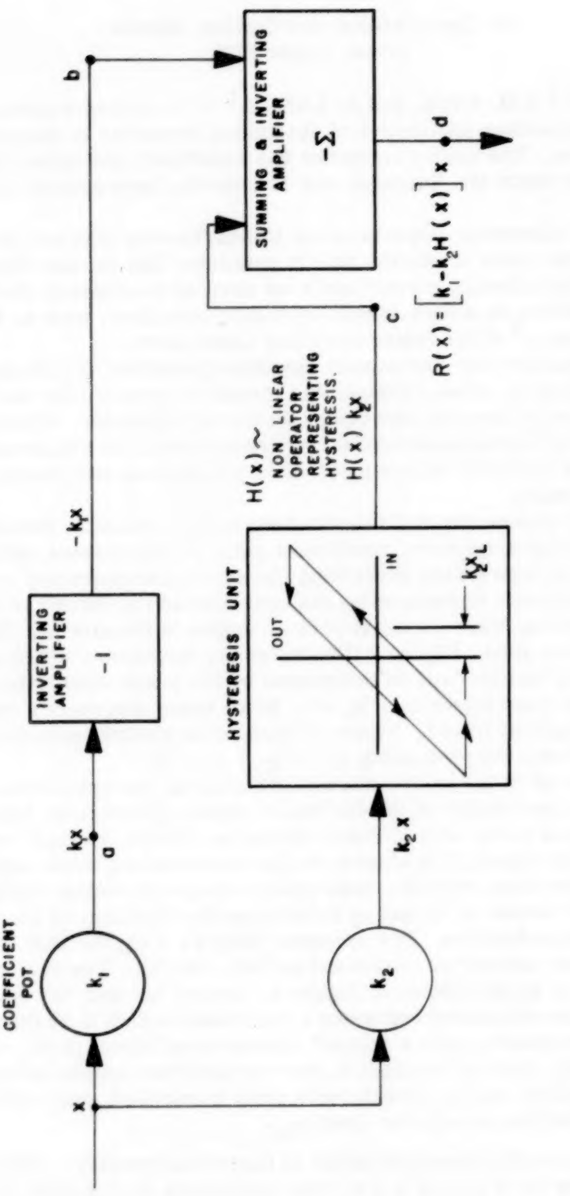
COEFFICIENT POT
x
k_1
k_1x
a
INVERTING AMPLIFIER
-1
$-k_1x$
b
SUMMING & INVERTING AMPLIFIER
$-\Sigma$
d
k_2
$k_2 x$
HYSTERESIS UNIT
OUT
IN
k_2X_L
$H(x) \sim$ NON LINEAR OPERATOR REPRESENTING HYSTERESIS.
$H(x)\ k_2x$
c
$R(x) = \left[k_1 - k_2H(x)\right] x$

FIG. — I

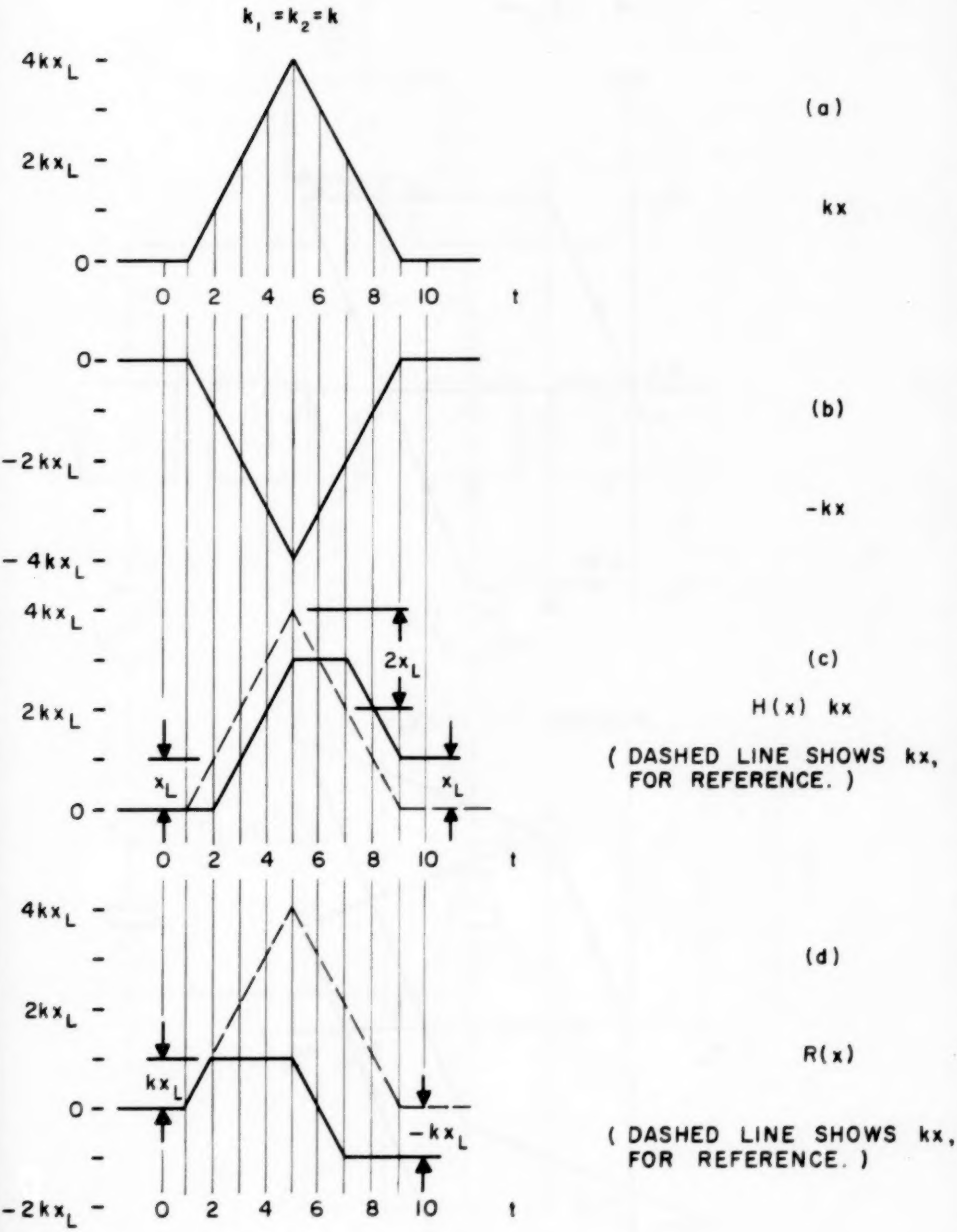
$k_1 = k_2 = k$
$4kx_L$
$2kx_L$
0
0 2 4 6 8 10 t
(a)
kx
$-2kx_L$
$-4kx_L$
(b)
-kx
$2x_L$
x_L
(c)
H(x) kx
(DASHED LINE SHOWS kx, FOR REFERENCE.)
kx_L
$-kx_L$
(d)
R(x)
(DASHED LINE SHOWS kx, FOR REFERENCE.)

FIG. — 2

$K_1 = K_2 = K$

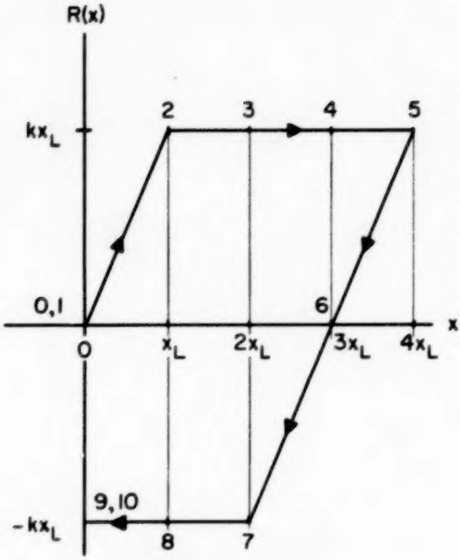

FIG. — 3

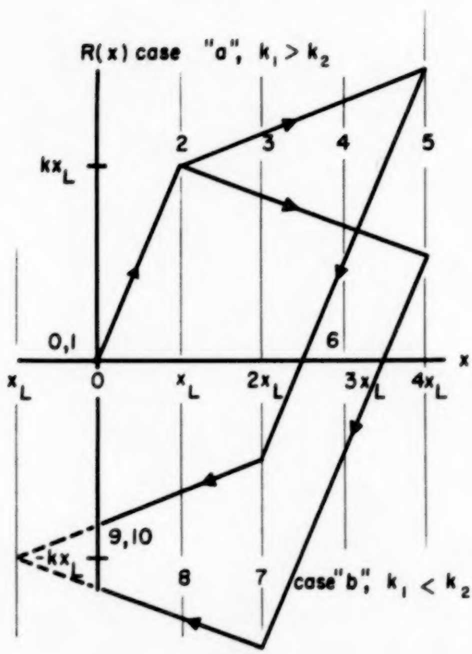

FIG. — 4

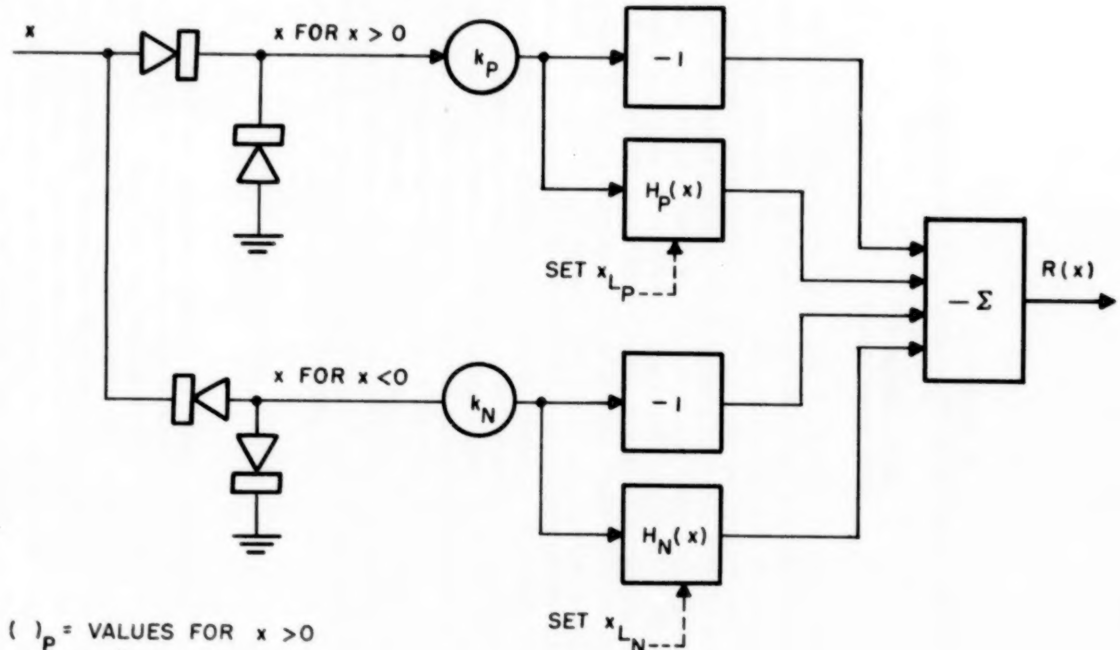

$(\ )_P$ = VALUES FOR $x > 0$
$(\ )_N$ = " " $x < 0$
k = ELASTIC COEFFICIENT
x_L = " LIMIT

FIG. – 5

Discussion of
"A NEW APPROACH TO TURBULENT BOUNDARY LAYER PROBLEMS"

by Donald Ross
(Proc. Paper 604)

W. DOUGLAS BAINES,[1] J.M. ASCE.—There are many cases of civil engineering work where a knowledge of behaviour of a turbulent boundary layer is important. Among these are conduit inlets in dams, entrances to tunnels, and streamlined struts immersed in water, the forces on which are primarily the result of surface friction. Open channel flow is a form of turbulent boundary layer and it can be shown to obey the same velocity distributions used by the author. Changes in flow regime are usually analysed by backwater computations but there are a few cases where a detailed knowledge of the flow is required. In such a case an analysis with the boundary layer equations must be made. The author has made an important contribution by simplifying the approach. He has eliminated the need for using differential equations and has presented useful graphs to support his analysis. However, before this method can be extensively used by civil engineers surface roughness must be considered because this is the most common case encountered. A similar analysis and a comparable series of curves must be prepared. It is to be hoped that this phase will be investigated in the near future.

The outer law for the velocity distribution as presented by the author is compatible with the commonly accepted law for the constant pressure case. Several investigators have studied this closely (Refs. 1 and 2) and find that the data are best represented by the following equation:

$$\frac{u_1 - u}{u^*} = f\left(\frac{y}{\delta}\right) \tag{A}$$

The function f has been found to be closely represented by a linear logarithmic law in the region between the edge of the laminar sub-layer and y/δ less than 0.15. This fact has been used (Ref. 1) to derive expressions for the wall shear coefficient for the flat-plate and circular-pipe cases. In each instance no blending region has been required to join the inner and outer velocity profiles. A question thus arises as to when a blending region is required. The author does not indicate how the blending region is defined. This is a serious omission because other investigators wishing to use his analysis will not have the benefit of his experience with the varied types of boundary-layer flow.

The right-hand side of equation (a) can readily be written as a function of $(1 - \frac{y}{\delta})$ which is the same variable found in the author's equation (7). It is significant that the function on the right-hand side can be represented by a power law. This has not been noted by other investigators and has lead to a considerable simplification in the analysis. In generalized form with the

1. Research Officer, National Research Council of Canada, Ottawa, Ontario.

power law variation, equation (A) can be written

$$1 - \frac{u}{u_1} = k\sqrt{\frac{c_f}{2}}\,(1 - \frac{y}{\delta})^m \qquad \text{(B)}$$

in which k and m are constant. Comparing equations (7) and (B) demonstrates that D is proportional to $\sqrt{\frac{c_f}{2}}$ for flat plates. The author infers that D is constant at a value about 0.3. This is correct for $R_\theta \approx 3000$ (a typical condition in wind tunnel investigations).

One point in which the writer does not agree is that the 3/2 power provides best fit to the experimental data. A value closer to 13/8 is better, as evidence note Figure A which is a log-log plot of some typical velocity profiles. For the outer 75% of the boundary layer the line of slope 1.625 is a very close fit. Similar agreement was found by the writer for the measurements of Sandborn and Slogar (Ref. 3) in an adverse pressure gradient. It thus appears that the analysis could be refined using a larger exponent. This, however, would not change any of the author's basic assumptions. The values of D in various equations and in Figures 7 through 12 would change thus necessitating a re-drafting of them. Use of a line of steeper slope on figures such as A results in a larger value of D for the same data.

Inasmuch as the detailed velocity distribution is not usually required in an analysis of the boundary layer, the suggested change would not produce significantly different results. The usual problem is to determine the boundary layers thickness, the friction drag or the point of separation. The author has based his curves on experimental evidence and as a result these quantities will be accurately predicted by his method.

It should be noted that equations (15) and (16) which refer to constant-pressure flow are not consistent. In equation (15) it is assumed that $\frac{\delta}{\theta D}$ is independent of x and as a result the differentiation is of θ alone. The final form of equation (15) gives A as a constant multiple of c_f. In the ensuing equation (16), A is given as an algebraic function of $\sqrt{c_f}$. The writer believes the explanation for this is that $\frac{\delta}{\theta D}$ is not constant but is also a function of c_f (and hence of x) as demonstrated by Landweber. The author's statement immediately preceding equation (16) is correct and has been demonstrated by Landweber who has shown that any mean-flow property of a turbulent boundary layer on a flat plate is a single value function of c_f. Unfortunately, most of the functions are so complicated that they are best presented graphically.

The writer hopes that the author's approach to turbulent boundary layer problems will receive attention from engineers working in this field so that its use in practical problems can be demonstrated.

REFERENCES

1. Landweber, L. "The Frictional Resistance of Flat Plates in Zero Pressure Gradient," Transactions, Society of Naval Architects and Marine Engineers, Vol. 61, 1953.

2. Baines, W. D. "A Literature Survey of Boundary-Layer Development on Smooth and Rough Surfaces at Zero Pressure Gradient," Iowa Institute of Hydraulic Research, 1951.

3. Sandborn, V. A. and Slogar, R. J. "Study of the Momentum Distribution of Turbulent Boundary Layers in Adverse Pressure Gradients," N.A.C.A. TN 3264, Jan. 1955.

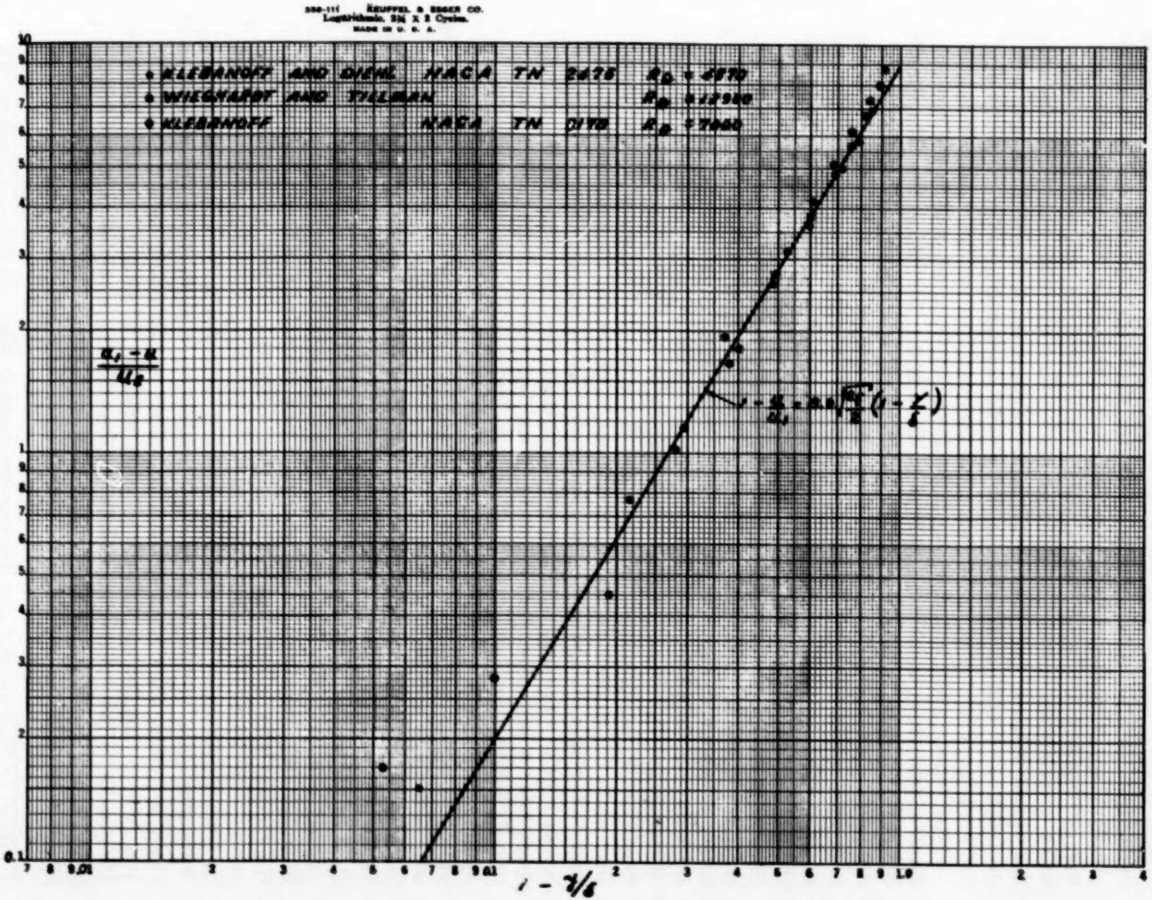

Figure A. Outer Law Velocity Distribution for Flat Plates.

J. M. ROBERTSON,[1] M. ASCE.—This paper represents an important step forward in our understanding of turbulent boundary layer flow. Having collaborated with Ross in other studies of this subject and having mildly kibitzed on the extensive study summarized in this paper, the writer may be biased in his assessment of the value of this paper—only time will tell. Fluid dynamics literature is replete with studies of the turbulent boundary layer in an adverse pressure gradient in which each investigator brought forth a new theory based on his experimental data only to have the next experimenter's work discredit it. Ross's study is on such a firm physical basis and utilizes the widest range of test data that it is to be expected to stand for some time. As implied by Ross a rigorous theory should appear eventually in terms of the statistical theory of turbulence—but that day appears to be far off.

Most work on the boundary layer problem has been devoted to the two-dimensional case, and many applications fall under this category. The three-dimensional case is naturally more complex but some applications (conical diffusers, flow about elongated bodies) can be treated as axisymmetric. This flow case might be termed quasi-two-dimensional as the flow is symmetrical about the flow-direction axis and only two coordinates are needed to describe the geometry. Ross's "approach" is for two-dimensional flow cases. It is natural to hope that it can be extended to the more general case—one wonders if it should not apply directly to the axisymmetric flow case which for relatively thin boundary layers is effectively two dimensional. Some studies of the axisymmetric boundary layer flow in a conical diffuser have been conducted at the Ordnance Research Laboratory of the Pennsylvania State University of E. M. Uram,[2] J. W. Holl, and the writer. These studies indicate that while the various relations introduced by Ross are most useful and effective for describing the flow the outer-profile parameter does not follow a linear type of variation with downstream distance. This might be expected from Ross's statement that equation 14 applies "provided the flow is very closely two-dimensional." Perhaps it may be possible to analyze the axisymmetric case in a manner similar to that used by Ross and obtain appropriate relations similar to equations 13 and 14. Until then empirical relations will have to do and we will have to consider the Ross approach to be limited strictly to the prediction of two-dimensional turbulent boundary layers in adverse pressure gradients.

It is unfortunate that this presentation of an exhaustive study had to be so greatly abbreviated. The writer hopes that Ross will rectify some of the more glaring omissions which occurred, for the benefit of those students of the subject who do not have ready access to the thick tome he wrote as a thesis. Not apparent in this paper is the complete physical background used by Ross in obtaining the relations used and the pains taken in sorting out, from that mass of data available on turbulent boundary layers, the most reliable sets of experimental information for use in verifying the analysis and determining the empirical constants needed. Certainly he should indicate the source of the experimental data and identify the symbols used to identify it in Figs. 9 and 10. For the benefit of completeness some indication of the criteria used in sorting out the experimental data used from that rejected

1. Prof. of Theoretical and Applied Mechanics, Univ. of Illinois, Urbana, Ill.
2. "The Growth of an Axisymmetric Turbulent Boundary Layer in an Adverse Pressure Gradient," E. M. Uram, to be published in Proc. of the Second U. S. National Congress for Applied Mechanics, 1955.

would be instructive and valuable. Certainly for any investigator planning further experimental research on this subject these would aid in proper design of experiments.

The division of the boundary layer flow into two regions—an inner wall region and an outer region relatively independent of local wall conditions—with some sort of a junction between them—is most important. In a sense the Law of the Wall concept for the inner region may be considered to have been initiated by Prandtl in stating that $u/u_* = \text{func}\ (yu_*/\nu)$ irrespective of just how far away the other side of the conduit is. Ross's contribution is that of analyzing the two basic regions completely separately. Not only does he indicate a unique relation for the inner region, as others have done, but he analyzes the outer flow region as a separate entity. All previous students of the subject have included the inner or wall region in their analysis of pressure gradient and history effects. The advantages of the new approach are evident in the paper.

In connection with the three-halves power deficiency law derived for the outer boundary layer region, it is interesting to note that Prandtl[(14)] in 1925 derived just such a law for the outer region in a pipe,

$$u = A - B\, r^{3/2}$$

where u is the velocity at radius r. In terms of the region in a pipe from the wall to the center line representing a boundary layer this is equivalent to equation 7 with $D = B\ \delta/u_1$. Prandtl's derivation was based on his momentum transfer theory with linear shear stress variation and constant mixing length—in exact accord with the indications of Fig. 3.

The linear shear stress variation in the outer region is justified as this quantity has been measured with hot-wire instrumentation.[(15)] The constancy of the mixing length in the outer region is not subject to explicit proof for this quantity cannot be measured directly. A few investigators have determined the mixing length by working back from velocity distributions with the aid of equation 11. Although this is subject to accumulated errors, the results indicate that the mixing length is essentially constant in the outer region. Thus Fig. A shows a universal plot of Nikuradse's[3] mixing length data for a family of diffusers. This plot was compiled by the writer a number of years ago[4] but no explanation for the arbitrary constant C was found. Actually 1/C is an indication of the fraction of the boundary layer influenced by the wall region. As Nikuradse's data is given at only one station in the diffuser, the manner in which the mixing length varies in the downstream direction is not clear. Evidence from other tests suggests that it may increase in the flow direction possibly directly with the boundary layer thickness. This uncertainty has been sidestepped by Ross in combining the mixing length in the outer region with other quantities to form a parameter whose form of variation in the flow direction he then infers by reference to experiment.

The writer has made a crude analysis of the longitudinal variation of the mixing length for the Schubauer and Klebanoff boundary layer[(15)] analyzed by Ross, with the results shown in Fig. B. The effective wall shear stress

---

3. "Untersuchunger über die Strömungen des Wassers in Konvergenten und Divergenten Kanälen," by J. Nikuradse, Forsch, VDI, Heft 289, 1929.
4. "Water Tunnel Diffuser Flow Studies, Part III - Analytical Research" by D. Ross and J. M. Robertson, Pennsylvania State University, Ord. Res. Lab., Report NOrd 7958-230, March 1952.

coefficient $c_{f_e} = \tau_{we}/\rho/2\, u_{1_i}^2$ has been estimated by extrapolation to the wall of the outer part of the lateral shear stress variations found by Schubauer and Klebanoff. From the equality in Ross's equation 13 and from the values of $\frac{\delta}{D}\left(\frac{u_{1_i}}{u_1}\right)$ given for this boundary layer in Fig. 7, the value of L has been computed. Both the effective wall shear stress and the mixing length in the outer region are seen to increase with distance in the flow direction at an increasing rate as separation is approached. The boundary layer thickness varies in about the same fashion and the ratio L/δ' of L to the thickness is seen to be nearly constant. (The boundary layer thickness δ' is the approximate outer limit indicated by Schubauer and Klebanoff for the layer.)

Numerous form parameters have been used for describing the shape of the velocity profile in turbulent flow. Ross's temerity in introducing yet another can only be justified by the observation made above that it is not only significant but unique in being limited to the description of the outer flow region irrespective of the flow in the inner wall region. The common shape parameter H is introduced (but not defined) in equation 8, the von Karman momentum integral equation. It is the ratio of the displacement thickness δ^* to the momentum thickness θ of the boundary layer. In two-dimensional flow δ^* is a measure of the amount the streamlines outside of the boundary layer region are laterally displaced due to the layer and the momentum thickness is a measure of the momentum deficiency in the layer. Because this parameter is so commonly used the writer strongly urges the author to present a graph indicating the relation between H and D even though H is not germane to his new approach. As H includes a description of the inner region as well as the outer region described by D, the Reynolds number or shear stress coefficient will presumably occur as a secondary parameter on such a graph. The various form parameters introduced into the literature up to about 1948 have been reviewed elsewhere[5] and their unsuitability for the analysis of the adverse pressure gradient case indicated.[6]

One form parameter introduced by Ludwieg and Tillmann[7] is $\gamma = \frac{u_1}{u_{\theta_e}}$ which Ross uses in his wall shear stress relations (equations 19 and 20) as well as equation 21. Thus equation 20 can be written

$$\sqrt{\frac{2}{c_f}} = \frac{1}{\gamma}\,(0.7 + 5.0 \log (R_\theta + \gamma))$$

But as γ is never greater than unity (cf Fig. 11) while R is large (> 100) we can write

5. "Water Tunnel Diffuser Flow Studies, Part I - Review of Literature," by J. M Robertson and D. Ross, Penn. State University, Ord. Res. Lab. Report NOrd 7958-139, May 1949.
6. "Water Tunnel Diffuser Flow Studies, Part III - Analytical Research," by D. Ross and J. M. Robertson, Penn. State University, Ord. Res. Lab., Report NOrd 7958-230, March 1952.
7. "Investigations of the Wall-Shearing Stress in Turbulent Boundary Layers," by H. Ludwieg and W. Tillmann, Ingenieur-Archiv, vol 17, 1949. (Translated in NACA Tech. Memo. 1285, 1950)

$$c_f = \frac{2\gamma^2}{(0.7 + 5.0 \log R_\theta)^2}$$

The skin friction coefficient can be expressed in terms of the value for a flat plate (zero pressure gradient) and γ. If we use the subscript o to indicate values which obtain without a pressure gradient then,

$$c_{f_o} = \frac{2\gamma_o^2}{(0.7 + 5.0 \log R_\theta)^2}$$

and we can write

$$c_f = \frac{\gamma^2}{\gamma_o^2} c_{f_o}$$

This type of relation was indicated by Ludwieg and Tillmann. Ross and Robertson (5) on the basis of a superposition analysis developed an equivalent relation,

$$c_f = (1-A')^2 \, c_{f_o}$$

in terms of A' the form parameter for the superposition analysis. A' must be related to γ by the relation

$$\gamma = \gamma_o \, (1-A)$$

A rough check on this for some diffuser data[8] is indicated in Fig. C. Since γ is correlated with D then A' must also be. Besides indicating the interrelationship of several form parameters this phase of the discussion suggests that the shear stress relation (equation 20) could be more simply expressed as

$$c_f = c_{f_o} \text{ func. } (D)$$

where the function of D could be given on a separate plot as a factor by which the flat plate drag is reduced due to the pressure gradient. This would permit those wishing to use a different flat plate drag law to take advantage of Ross's analysis of the pressure gradient effect.

In any analysis of the turbulent boundary layer in an adverse pressure gradient a very important consideration is the occurrence of separation or how close one comes to it. The writer is not particularly convinced that in stating D = 1.3 is the criterion for separation that Ross has improved on other criteria such as H = 2.5, A' = 0.8, etc. The only improvement is that D typifies the outer flow region, and as noted by Prandtl in 1904 "the flow separates

8. "Effect of Entrance Conditions on Diffuser Flow," by J. M. Robertson and D. Ross, Trans. ASCE, vol 118, p 1068, 1953.

from the surface at a point entirely determined by external conditions."(2)[9]

As a means for analyzing boundary layer progression in an adverse pressure gradient, the new approach can be used to predict the growth and eventual separation of the layer for a given flow condition. Not only this but it can be used to ascertain how much a given boundary layer can be decelerated before it separates without performing the necessary calculations on the growth, i.e., in terms of the terminal conditions alone. As indicated by Ross (private communication) equation 17 can be used to indicate which flows will proceed towards separation and which will not. Usually one wishes the flow to proceed close to separation without it occurring. With the aid of equation 9 one can write equation 17 as

$$f = (A \frac{\Delta x}{\theta_1} + f_1)(\frac{u_1}{u_{1_1}})^{3+G}$$

where f = func. (D) = $\delta\,\theta/D$ and f_1 is the initial value. Taking D = 1.3 for separation the left side of the equation is f = 5 (according to Fig. 10). The initial value f_1 is also obtained from the initial value of D, which is approximately 0.3, for a flow starting from flat plate conditions. In his thesis Ross shows that D in flat plate flow varies slowly with Reynolds number. This variation is enough to significantly affect the present solution. The writer had the thesis available—for the benefit of others he would suggest that Ross include a presentation of this variation in his concluding discussion. The constant A is a function of the momentum thickness Reynolds number (cf equation 16) as is also the exponent (3 + G) (cf Fig. 5). The above equation has been solved for the allowable reduction in u_1 for three different values of the initial momentum thickness Reynolds number, for which the various constants are indicated in Table I. With n = 1/(G + 3) the equation may be written,

$$\frac{u_1}{u_{1_1}} = (\frac{5}{A\frac{\Delta x}{\theta_1} + f_1})^n$$

As the relations are not applicable for $\Delta x/\theta_1$ greater than 50 and because of the relative magnitudes of A and f_1 listed in the

TABLE I

R_{θ_1}	D_i	f_1	c_f	A	n
10^3	0.384	21.7	0.00465	0.0454	0.166
10^4	0.312	30	0.0026	0.0403	0.183
10^5	0.254	43	0.0016	0.037	0.193

table, the relation can be written (with an error less than 2 percent) as

$$\frac{u_1}{u_{1_1}} = (\frac{5}{f_1})^n$$

9. See also translation in NACA Tech. Memo. 452, 1928.

The solution of this relation is presented in Fig. D which shows the permissible decrease in velocity (without separation) as a function of the initial Reynolds number. Also shown is a more conservative solution with D = 1.0 for which f = 6.1.

Three conclusions are indicated by the above calculation. Firstly, that the allowable deceleration is not great. Second, that how fast you get there does not matter (as the results are independent of x). And thirdly, for higher Reynolds numbers there is less chance of separation. It must be recalled that these conclusions are limited by the limits of equation 9 (cf Ref. 17) and an x limit of $50\theta_1$. As the first two conclusions were somewhat beyond the writer's expectation a search was made for possible experimental verification. Two series of experiments were checked: the NBS work by Schubauer and Klebanoff(15) and work at Sidney University by Newman.[10] These two points are plotted on Fig. D showing in the NBS case excellent agreement but an underprediction in the case of the SU work. The writer would appreciate Ross's comments on this analysis as well as an indication of other uses of equation 17 to predict overall flow conditions.

W. J. BAUER,[11] J.M. ASCE.—This discussion will be limited to a comparison of the shape of the empirical velocity profile proposed by the author with measurements made by the writer in a steep laboratory flume.[12] The comparison is presented graphically in Figs. 13 and 14.

In Fig. 13 u/u_* is plotted on a linear ordinate scale as a function of yu_*/ν plotted on a logarithmic abscissa scale. On the same field a straight line has been drawn to represent Ludweig's Law of the Wall as given by the author in equation 6. Although the author states that this function is valid for y/δ less than 0.1, points have been plotted for y/δ values up to 0.25. The seven velocity profiles presented were selected at random from a group of 30-odd profiles measured by the writer[13] above the plate glass floor of a steep laboratory flume. Except for the one profile obtained on the 40^o slope at $\delta u_1/\nu = 2.14 \times 10^5$, the points appear to be reasonably well bunched and in fair agreement with equation 6. Slight adjustment of the constant of equation 6 would obviously give a better fit, however. (In this connection, it is to be noted that equation 6 is also known as the Karman-Prandtl velocity-distribution equation for flow in pipes, albeit with slightly different values of A and B.)[14] One may conclude that the inner portion of the velocity profiles on steep slopes are adequately described by the author's proposed approximation.

In Fig. 14, the outer portions of the same seven profiles do not appear to be as well approximated by equation 7 which the author proposes to describe

10. "Some Contributions to the Study of the Turbulent Boundary-Layer Near Separation," by B. G. Newman, Aeronautical Research Consultative Committee, Australia, Report ACA-53, March 1951.
11. Senior Designer, Harza Eng. Co., Chicago, Ill.
12. Bauer, "The Development of the Turbulent Boundary Layer on Steep Slopes," Transactions ASCE, Vol. 119, 1954, p. 1212.
13. Bauer, "The Development of the Turbulent Boundary Layer on Steep Slopes," a dissertation submitted in partial fulfillment of the requirements for the degree of Doctor of Philosophy, in the Department of Mechanics and Hydraulics, in the Graduate College of the State University of Iowa, August, 1951.
14. Rouse, Hunter, M. ASCE, "Elementary Mechanics of Fluids," John Wiley & Sons, Inc., 1946.

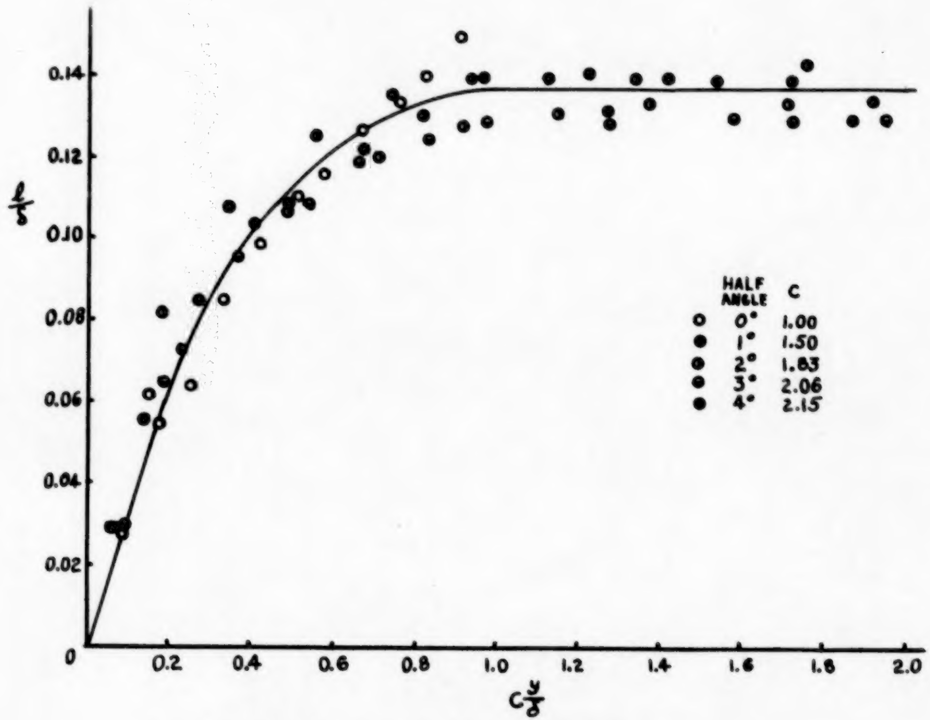

FIG A UNIVERSAL PLOT OF MIXING LENGHS FROM NIKURADSE'S DIFFUSER STUDY

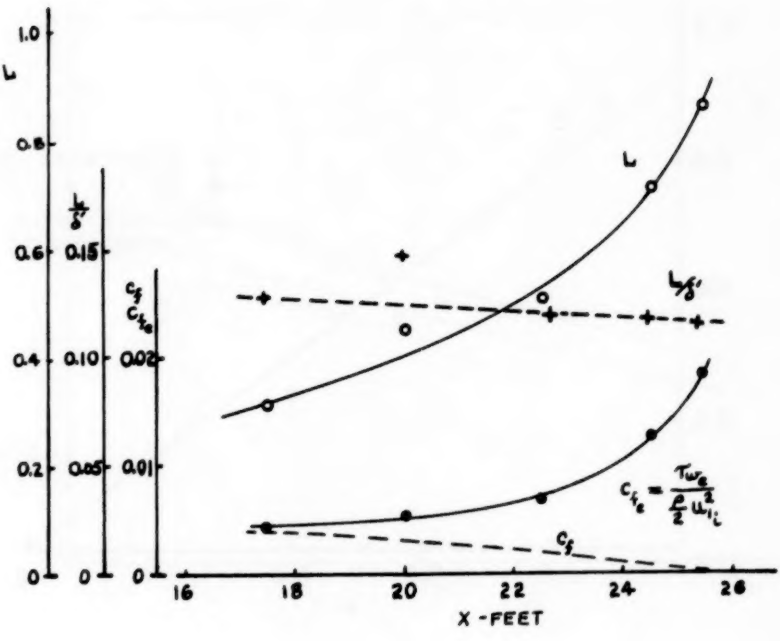

FIG B LONGITUDINAL VARIATION IN OUTER MIXING LENGTH - SCHUBAUER AND KLEBANOFF BOUNDARY LAYER

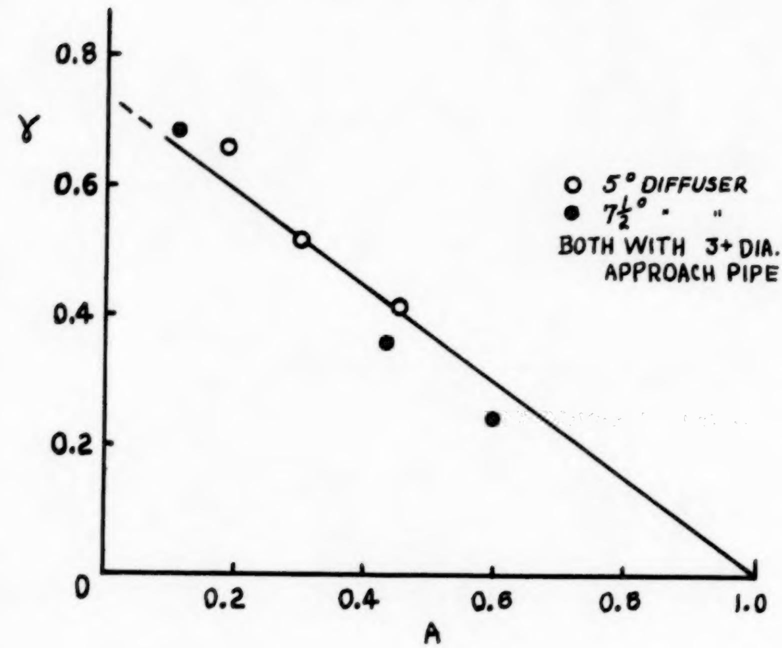

FIG C CORRELATION BETWEEN SHAPE PARAMETERS A AND γ.

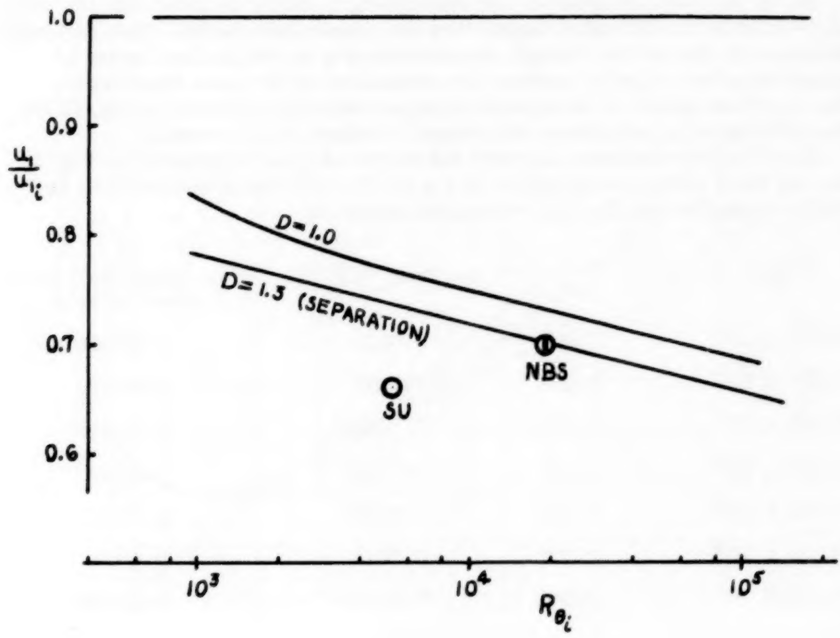

FIG D PERMISSIBLE VELOCITY DECREASE WITHOUT SEPARATION AS A FUNCTION OF INITIAL REYNOLDS NUMBER.

the shape of the outer 75% of the profile. The values of D presented here were computed from equation 7 for known values of the remaining variables. Even within the limits proposed by the author, the value of D varies rather widely, particularly for values of y/δ greater than 0.7. Nevertheless, the value of D is relatively constant in the middle 40% of the profile, and it can be shown that the use of an average value obtained from this region will result in a reasonably good approximation of the velocity profile outside of this range due to the nature of the function. No apparent systematic variation with slope or location on the flume is evident in Fig. 14. Thus it appears that equation 7 is also a useful description of the shape of the velocity profile within turbulent boundary layers on steep slopes.

As far as rough boundaries are concerned, it should be noted that the value of D would be considerably larger than for smooth boundaries. This fact was evaluated by the writer through examination of a corresponding series of rough-boundary velocity profiles also measured in the same steep flume. The D values appear to be about 0.15 larger than those plotted in Fig. 14 for the corresponding conditions on a rough boundary of flyscreen.

As a final comparison, consider the values of c_f as obtained from Fig. 12 (on the basis of measured values of R_θ and D) with values computed by the writer using the von Karman momentum equation:

R_θ	D	c_f from Fig. 12	c_f from writer's computations
1.63×10^4	0.24	0.0025	0.00265
1.07×10^4	0.25	0.0027	0.00275
0.46×10^4	0.27	0.00315	0.00315
2.00×10^4	0.24	0.0024	0.0028
0.64×10^4	0.28	0.00295	0.0031
2.04×10^4	0.23	0.0025	0.0025
0.72×10^4	0.27	0.00295	0.00295

The D values are averages from the middle 40% of the profiles.

The writer congratulates the author for a straightforward presentation of a relatively simple and apparently useful approximation of the turbulent boundary-layer velocity profile. Although his work will find its most frequent application to the calculation of boundary layers with adverse pressure gradients, the author has nevertheless presented a method which is equally valid for developments in accelerating flow.

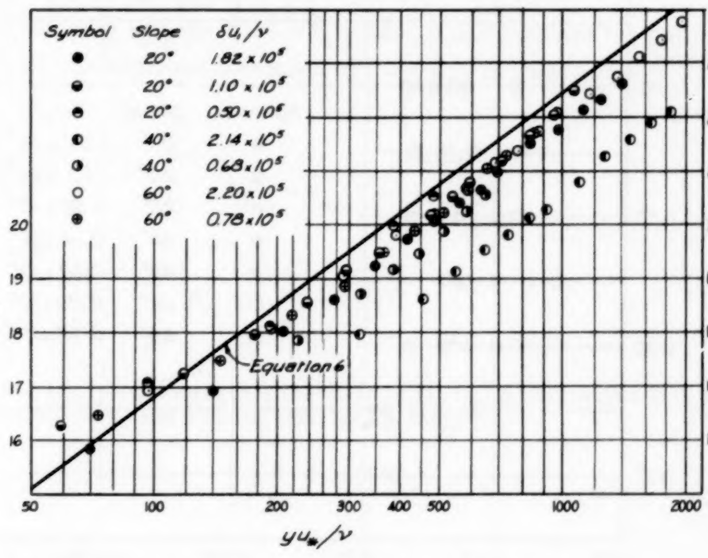

Fig. 13. The Law of the Wall for Steep Slopes.

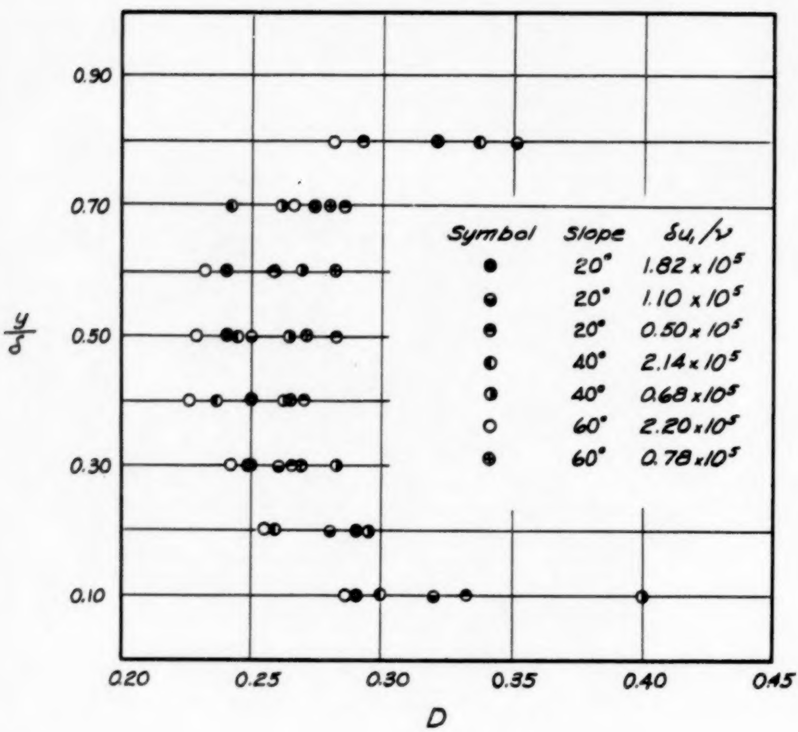

Fig. 14. Variation of D on Steep Slopes.

Discussion of
"LATERAL BUCKLING OF ECCENTRICALLY LOADED I-COLUMNS"

by Mario G. Salvadori
(Proc. Paper 607)

CORRECTIONS—

a) From Eq. (35) on p. 607-9 to first sentence after Eq. (39), substitute:
"In order to take into account the reduction of torsional rigidity in the evaluation of the interaction curves, H must be substituted for C in Eq. (30), both in $\sqrt{BC}$ and in $k_{0,1}$.
Indicating by $k'_{0,1}$ the value of $k_{0,1}$ when H is substituted for C in ℓ^2/a^2, the relationship between $k'_{0,1}$ and $k_{0,1}$ is found to be:

$$k'_{0,1} = k_{0,1} \frac{\sqrt{1 - P/P_{T1}}}{\sqrt{1 - P/P_T}} \quad [4] \tag{36}$$

where:

$$P_{T1} = P_T \left[1 + \left(\frac{\pi}{\ell/a}\right)^2\right] \tag{37}$$

Similarly, indicating by M'_2 the value of M_2 in Eq. (30) where H is substituted for C, and noticing that, by Eq. (35):

$$\sqrt{\frac{H}{C}} = \sqrt{1 - P/P_T} ,$$

it is found that:

$$M'_2 = K_r \bar{\mu}_r k'_{0,1} \frac{\sqrt{BH}}{\alpha L}$$

$$= K_r \bar{\mu}_r k_{0,1} \frac{\sqrt{BC}}{\alpha L} \sqrt{1 - P/P_{T1}}$$

or, by Eq. (13), that:

$$K'_r = \frac{M'_2}{M_{0,2}} = K_r \sqrt{1 - P/P_{T1}}$$

4. This result is in agreement with the theoretical results in ref. 5 and with the experimental results of ref. 8.

By means of the parameter:

$$\gamma = \frac{P_{cr.}}{P_{T1}} = \frac{\pi^2 B I_p}{\alpha^2 L^2 CA \left(1 + \frac{\pi^2 a^2}{\alpha^2 L^2}\right)} \tag{38}$$

K_r' may be written as:

$$K_r' = K_r \sqrt{1 - \gamma p} \quad . \tag{39}$$

The parameter γ varies, practically, between zero and one.

b) Delete note 4 on p. 607-9

c) Add to list of references:
8. Hill, H. N. and Clark, J. W., "Lateral Buckling of Eccentrically loaded I-Section Columns," Transactions ASCE, Vol. 116, 1951, p. 1179.

d) In Fig. 3: heavy lines $\frac{P_{cr}}{P_{T1}} = 1.0$; light lines $\frac{P_{cr.}}{P_{T1}} = 0$.

e) Equation (24) should read:

$$P = \frac{C}{2e^2} \left(\frac{k_{0,1}}{\pi} \right)^2 \left[-1 + \sqrt{1 + \frac{4\pi^2}{\alpha^2} \frac{Be^2}{CL^2} \left(\frac{\pi}{k_{0,1}} \right)^2} \right]$$

f) Line after Eq. (31), end of line:

$$M_2 = K_r \sqrt{B C} / L$$

Discussion of
"FAILURE OF PLAIN CONCRETE UNDER COMBINED STRESSES"

by Boris Bresler and Karl S. Pister
(Proc. Paper 674)

PAUL RICE,[1] J.M. ASCE.—Data on the combination of tensile and compressive principal stresses were given in "Failure of Concrete Under Combined Tensile and Compressive Stresses," G. M. Smith, Journal of the American Concrete Institute, October, 1953, No. 50-8. The purposes of this discussion are (1) to correlate this additional experimental data and (2) to correlate data given by the authors with a suggested design equation given in the earlier paper.

The results in Smiths' paper agreed well with a simple design formula:

$$\left(\frac{\sigma_1}{M_R}\right)^2 + \left(\frac{-\sigma_3}{f'_c}\right)^2 = 1$$

in which: σ_1, $-\sigma_3$ - are principal stresses

M_R - modulus of rupture

f'_c - ultimate compressive strength (standard cylinder test)

The results (scaled from the plotted data) when plotted as dimensionless ratios $(-\tau_o/f'_c)$ and (σ_o/f'_c), in which τ_o and σ_o are the octahedral shear and normal stresses respectively, give a close agreement with the authors' equation (6) for a criterion of failure. A comparison shows:

Authors' equation (6): $-\left(\tau_o/\sigma_c\right) = 1.15\left(\frac{\sigma_o}{\sigma_c}\right) - 0.087$

Data from Smith: $\left(-\tau_o/f'_c\right) = 1.15\left(\sigma_o/f'_c\right) - 0.115$

Converting to the authors' notation (taking $\sigma_c = (0.866)\ (1.06)\ f'_c$ since the authors state that σ_c is taken as 86.6% of 3x6 cylinder strengths which are 106% f'_c based on standard cylinders) we get: $-(\tau_o/\sigma_c) = 1.15\ (\sigma_o/\sigma_c) - 0.125$. See figure 1.

A possible explanation for the difference in constants (in addition to errors in measurement, etc.) is that Smith's data are based upon tension calculated as Mc/I for beams in flexure. "Modulus of rupture" so calculated usually differs from tensile strength determined by direct tensile test.

Using the average values for compressive $(-\sigma)$ and shearing (τ) stresses at failure as given in the authors' Table 1, principal stresses (σ_1) and $(-\sigma_3)$

1. Technical Director, American Concrete Inst., Detroit, Mich.

were calculated. A comparison of these values to a curve for Smith's equation, using the common approximation for ultimate tensile strength, $f'_t = 0.10\, f'_c$, is shown in Fig. 2. The resulting design formula is:

$$\left(\frac{\sigma_1}{0.10\, f'_c}\right)^2 + \left(\frac{-\sigma_3}{f'_c}\right)^2 = 1$$

It should be noted that this equation provides a rational pattern for the data shown in the authors' Fig. 3, and is presented in a form convenient for the use of, and familar to, structural designers.

FRANK A. BLAKEY[2] and F. D. BERESFORD.[3]—The writers have done numerous tests on plain concrete beams, discs and slabs arranged so that the failure under uniaxial tension, equal tensions at right angles and equal compression and tension at right angles of concrete could be studied. The full details of these tests are given elsewhere.(1,2)[4] As a result of these tests the law governing the fracture of concrete was proposed in the form:-

$$I_1^2 - 2I_2 + 2.4\tau_b . I_1 = 3.4\tau_b^2 \quad \ldots\ldots\ldots \text{(A)}$$

where I_1 and I_2 are the first and second stress invariants and τ_b is the failure stress of concrete in bending in beams.

Equation (6) of Bresler and Pister may be put to the form

$$I_1^2 - 9.18I_2 + 9.18\tau_b I_1 = 10.4\tau_b^2 \quad \ldots\ldots \text{(B)}$$

if it is assumed that $\sigma_c = -10\,\tau_b$.

This assumption is supported by the results in Fig. 3, but any other assumed ratio for σ_c and τ_b would only alter the coefficients of the terms $\tau_b I_1$ and τ_b^2 in the latter expression but not change the agreement in general form between the hypothesis of the authors and the present writers.

This agreement in form can be further demonstrated if the physical interpretation of the stress invariants is considered.

If e is the volumetric strain or dilatation and U_s is the shear strain energy, or energy of change of shape, then it can be shown that

$$U_s = \frac{1+\mu}{3E}(I_1^2 - 3I_2)$$

and

$$e = \frac{1-2\mu}{E} . I_1$$

where E and μ are the elastic constants.

---

2. Senior Research Officer, Div. of Building Research, Commonwealth Scientific and Industrial Research Organization, Melbourne, Australia.
3. Technical Officer, Div. of Building Research, Commonwealth Scientific and Industrial Research Organization, Melbourne, Australia.
4. Numbers refer to references at the end of discussion.

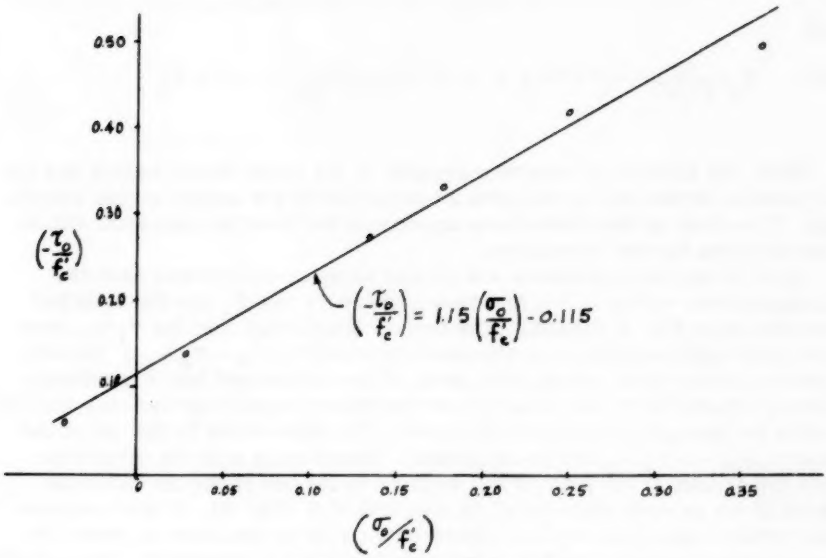

Fig. 1 - Data By G. M. Smith.

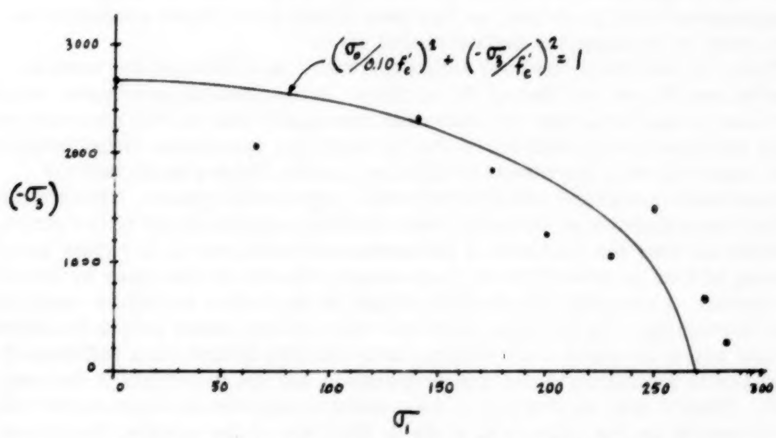

Fig. 2 - Principal Stresses (Authors' Data for Their Fig. 3).

If these relationships are substituted in equations (A) and (B) it will be found that:

$$(A1) \quad U_s . \frac{3E}{1+\mu} + I_2 + 2.4\tau_b . \frac{Ee}{1-2\mu} = 3.4\tau_b^2$$

and

$$(B1) \quad U_s . \frac{3E}{1+\mu} - 6.18I_2 + 9.18\tau_b . \frac{Ee}{1-2\mu} = 10.4\tau_b^2$$

Thus, the fracture of concrete depends on the shear strain energy and the volumetric strain and an odd term associated with the second stress invariant. The effect of this latter form appears to be the most important difference between the two hypotheses.

Again if the two hypotheses are plotted using as co-ordinate axes the dimensionless ratios τ_1/τ_b and τ_2/τ_b where τ_1 and τ_2 are the principal stresses then Fig. A results. (The results are plotted only for τ_1/τ_b positive since both equations are symmetrical about $\tau_1/\tau_b = \tau_2/\tau_b$.) The differences in the first and adjacent parts of the second and fourth quadrants, although fairly large are probably not practically significant and may well be within the margin of experimental error. The differences to the left of the line $\tau_1/\tau_b = - \tau_2/\tau_b$ are much greater. However, it must be noted here that the results of the authors fall entirely to the left of the line whereas those of the present writers fall to the right of it (Fig. A). In their reports the writers emphasize that the choice of a circle as the curve to which the experimental points were fitted was based only on its simplicity. It was fully realized that further work might show other curves to be more suitable, but as it was realized that any other second degree curve would be capable of the same physical interpretation, as has been shown here, there seemed to be little point in pursuing the matter at that stage.

There is, however, one very important difference between the work of Bresler and Pister and that of the writers. In the flexural specimens which they used it was found that microcracks developed—that is, the concrete material failed—at loads well below that at which the specimens ultimately fell apart, and it is with the stress conditions causing these cracks that the writers were concerned and to which their hypothesis applies. These microcracks were discovered through a very detailed measurement of the strain distribution over the surfaces of the specimens used, and it is rather disappointing to find no reference to strain measurements in the paper by Bresler and Pister. A complete study of the strain in the hollow cylinders would have been interesting. On the other hand the writers have some reason to believe that the extent to which these microcracks develop before final collapse of a specimen is a function of the mix proportions and the materials of the concrete. Thus it may be that the close qualitative agreement between the two hypotheses is an indication that while in the tests of the writers the microcracks developed at loads well below failure, in the tests of the authors they developed at loads very close to failure.

REFERENCES

1. Blakey, F. A. and Beresford, F. D., "Tensile Strains in Concrete" Part I. C.S.I.R.O. Division of Building Research Report C2.2-1 (1953).

2. Blakey, F. A. and Beresford, F. D., "Tensile Strains in Concrete" Part II. C.S.I.R.O. Division of Building Research Report C2.2-2 (1955).

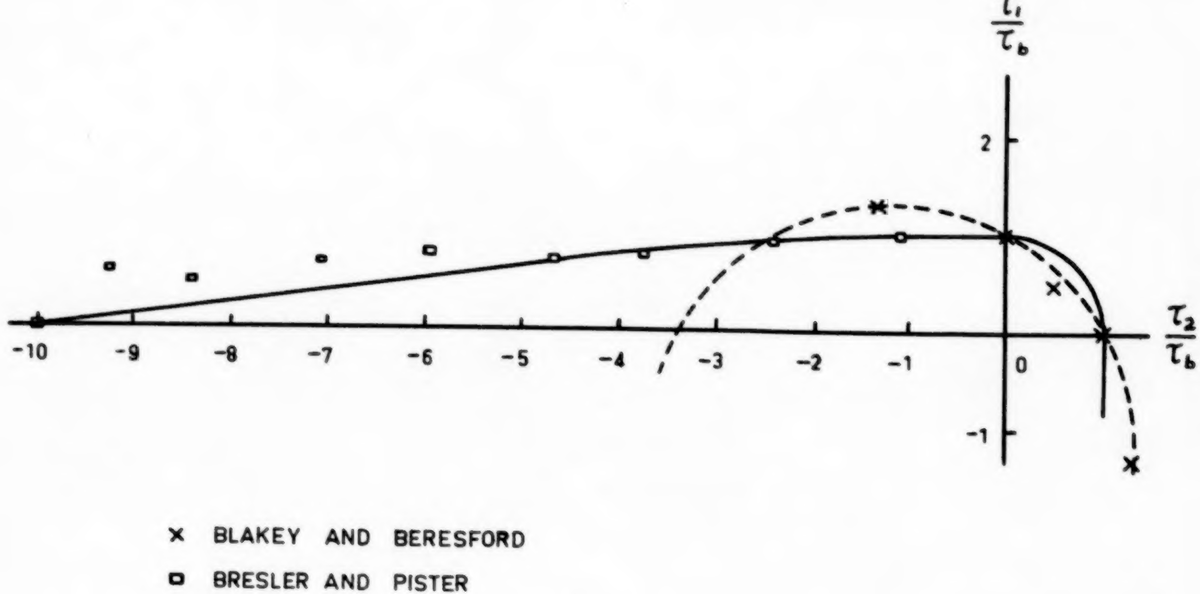

$\frac{\tau_1}{\tau_b}$
$\frac{\tau_2}{\tau_b}$
2
-1
-10
-9
-8
-7
-6
-5
-4
-3
-2
-1
0
× BLAKEY AND BERESFORD
▫ BRESLER AND PISTER

Fig. A.

PROCEEDINGS PAPERS

The technical papers published in the past year are presented below. Technical-division sponsorship is indicated by an abbreviation at the end of each Paper Number, the symbols referring to: Air Transport (AT), City Planning (CP), Construction (CO), Engineering Mechanics (EM), Highway (HW), Hydraulics (HY), Irrigation and Drainage (IR), Power (PO), Sanitary Engineering (SA), Soil Mechanics and Foundations (SM), Structural (ST), Surveying and Mapping (SU), and Waterways (WW) divisions. For titles and order coupons, refer to the appropriate issue of "Civil Engineering" or write for a cumulative price list.

VOLUME 80 (1954)

AUGUST: 466(HY), 467(HY), 468(ST), 469(ST), 470(ST), 471(SA), 472(SA), 473(SA), 474(SA), 475(SM), 476(SM), 477(SM), 478(SM)[c], 479(HY)[c], 480(ST)[c], 481(SA)[c], 482(HY), 483(HY).

SEPTEMBER: 484(ST), 485(ST), 486(ST), 487(CP)[c], 488(ST)[c], 489(HY), 490(HY), 491(HY)[c], 492(SA), 493(SA), 494(SA), 495(SA), 496(SA), 497(SA), 498(SA), 499(HW), 500(HW), 501(HW)[c], 502(WW), 503(WW), 504(WW)[c], 505(CO), 506(CO)[c], 507(CP), 508(CP), 509(CP), 510(CP), 511(CP).

OCTOBER: 512(SM), 513(SM), 514(SM), 515(SM), 516(SM), 517(PO), 518(SM)[c], 519(IR), 520(IR), 521(IR), 522(IR)[c], 523(AT)[c], 524(SU), 525(SU)[c], 526(EM), 527(EM), 528(EM), 529(EM), 530(EM)[c], 531(EM), 532(EM)[c], 533(PO).

NOVEMBER: 534(HY), 535(HY), 536(HY), 537(HY), 538(HY)[c], 539(ST), 540(ST), 541(ST), 542(ST), 543(ST), 544(ST), 545(SA), 546(SA), 547(SA), 548(SM), 549(SM), 550(SM), 551(SM), 552(SA), 553(SM)[c], 554(SA), 555(SA), 556(SA), 557(SA).

DECEMBER: 558(ST), 559(ST), 560(ST), 561(ST), 562(ST), 563(ST)[c], 564(HY), 565(HY), 566(HY), 567(HY), 568(HY)[c], 569(SM), 570(SM), 571(SM), 572(SM)[c], 573(SM)[c], 574(SU), 575(SU), 576(SU), 577(SU), 578(HY), 579(ST), 580(SU), 581(SU), 582(Index).

VOLUME 81 (1955)

JANUARY: 583(ST), 584(ST), 585(ST), 586(ST), 587(ST), 588(ST), 589(ST)[c], 590(SA), 591(SA), 592(SA), 593(SA), 594(SA), 595(SA)[c], 596(HW), 597(HW), 598(HW)[c], 599(CP), 600(CP), 601(CP), 602(CP), 603(CP), 604(EM), 605(EM), 606(EM)[c], 607(EM).

FEBRUARY: 608(WW), 609(WW), 610(WW), 611(WW), 612(WW), 613(WW), 614(WW), 615(WW), 616(WW), 617(IR), 618(IR), 619(IR), 620(IR), 621(IR)[c], 622(IR), 623(IR), 624(HY)[c], 625(HY), 626(HY), 627(HY), 628(HY), 629(HY), 630(HY), 631(HY), 632(CO), 633(CO).

MARCH: 634(PO), 635(PO), 636(PO), 637(PO), 638(PO), 639(PO), 640(PO), 641(PO)[c], 642(SA), 643(SA), 644(SA), 645(SA), 646(SA), 647(SA)[c], 648(ST), 649(ST), 650(ST), 651(ST), 652(ST), 653(ST), 654(ST)[c], 655(SA), 656(SM)[c], 657(SM)[c], 658(SM)[c].

APRIL: 659(ST), 660(ST), 661(ST)[c], 662(ST), 663(ST), 664(ST)[c], 665(HY)[c], 666(HY), 667(HY), 668(HY), 669(HY), 670(EM), 671(EM), 672(EM), 673(EM), 674(EM), 675(EM), 676(EM), 677(EM), 678(HY).

MAY: 679(ST), 680(ST), 681(ST), 682(ST)[c], 683(ST), 684(ST), 685(SA), 686(SA), 687(SA), 688(SA), 689(SA)[c], 690(EM), 691(EM), 692(EM), 693(EM), 694(EM), 695(EM), 696(PO), 697(PO), 698(SA), 699(PO)[c], 700(PO), 701(ST)[c].

JUNE: 702(HW), 703(HW), 704(HW)[c], 705(IR), 706(IR), 707(IR), 708(IR), 709(HY)[c], 710(CP), 711(CP), 712(CP), 713(CP)[c], 714(HY), 715(HY), 716(HY), 717(HY), 718(SM)[c], 719(HY)[c], 720(AT), 721(AT), 722(SU), 723(WW), 724(WW), 725(WW), 726(WW)[c], 727(WW), 728(IR), 729(IR), 730(SU)[c], 731(SU).

JULY: 732(ST), 733(ST), 734(ST), 735(ST), 736(ST), 737(PO), 738(PO), 739(PO), 740(PO), 741(PO), 742(PO), 743(HY), 744(HY), 745(HY), 746(HY), 747(HY), 748(HY)[c], 749(SA), 750(SA), 751(SA), 752(SA)[c], 753(SM), 754(SM), 755(SM), 756(SM), 757(SM), 758(CO)[c], 759(SM)[c], 760(WW)[c].

AUGUST: 761(BD), 762(ST), 763(ST), 764(ST), 765(ST)[c], 766(CP), 767(CP), 768(CP), 769(CP), 770(CP), 771(EM), 772(EM), 773(SA), 774(EM), 775(EM), 776(EM)[c], 777(AT), 778(AT), 779(SA), 780(SA), 781(SA), 782(SA)[c], 783(HW), 784(HW), 785(CP), 786(ST).

c. Discussion of several papers, grouped by Divisions.

AMERICAN SOCIETY OF CIVIL ENGINEERS

OFFICERS FOR 1955

PRESIDENT

WILLIAM ROY GLIDDEN

VICE-PRESIDENTS

Term expires October, 1955:
ENOCH R. NEEDLES
MASON G. LOCKWOOD

Term expires October, 1956:
FRANK L. WEAVER
LOUIS R. HOWSON

DIRECTORS

Term expires October, 1955:
CHARLES B. MOLINEAUX
MERCEL J. SHELTON
A. A. K. BOOTH
CARL G. PAULSEN
LLOYD D. KNAPP
GLENN W. HOLCOMB
FRANCIS M. DAWSON

Term expires October, 1956:
WILLIAM S. LaLONDE, JR.
OLIVER W. HARTWELL
THOMAS C. SHEDD
SAMUEL B. MORRIS
ERNEST W. CARLTON
RAYMOND F. DAWSON

Term expires October, 1957:
JEWELL M. GARRELTS
FREDERICK H. PAULSON
GEORGE S. RICHARDSON
DON M. CORBETT
GRAHAM P. WILLOUGHBY
LAWRENCE A. ELSENER

PAST-PRESIDENTS

Members of the Board

WALTER L. HUBER
DANIEL V. TERRELL

EXECUTIVE SECRETARY

WILLIAM H. WISELY

TREASURER

CHARLES E. TROUT

ASSISTANT SECRETARY

E. L. CHANDLER

ASSISTANT TREASURER

CARLTON S. PROCTOR

PROCEEDINGS OF THE SOCIETY

HAROLD T. LARSEN
Manager of Technical Publications

DEFOREST A. MATTESON, JR.
Editor of Technical Publications

PAUL A. PARISI
Assoc. Editor of Technical Publications

COMMITTEE ON PUBLICATIONS

SAMUEL B. MORRIS, *Chairman*

JEWELL M. GARRELTS, *Vice-Chairman*

GLENN W. HOLCOMB
OLIVER W. HARTWELL

ERNEST W. CARLTON
DON M. CORBETT